

Revealing the Source of the Radial Flow Patterns in Proton-Proton Collisions using Hard Probes

Antonio Ortiz¹, Gyula Bencédi^{1,3}, Héctor Bello^{1,2}

¹ Instituto de Ciencias Nucleares, UNAM, México City, México

² Facultad de Ciencias Físico Matemáticas, BUAP, 1152, Puebla, México

³ Wigner Research Centre for Physics of the HAS, Budapest, Hungary

E-mail: bencedi.gyula@wigner.mta.hu

Abstract.

In this work, we propose a tool to reveal the origin of the collective-like phenomena observed in proton–proton collisions. We exploit the fundamental difference between the underlying mechanisms, color reconnection (CR) and hydrodynamics, which produce radial flow patterns in PYTHIA 8 and EPOS 3, respectively. Specifically, we proceed by examining the strength of the coupling between the soft and hard components which, by construction, is larger in PYTHIA 8 than in EPOS 3.

We study the transverse momentum (p_T) distributions of charged pions, kaons and (anti)protons in inelastic pp collisions at $\sqrt{s} = 7$ TeV produced at mid-rapidity. Specific selections are made on an event-by-event basis as a function of the charged particle multiplicity and the transverse momentum of the leading jet (p_T^{jet}) reconstructed using the FASTJET algorithm at mid-pseudorapidity ($|\eta| < 1$). From our studies, quantitative and qualitative differences between PYTHIA 8 and EPOS 3 are found in the p_T spectra when (for a given multiplicity class) the leading jet p_T is increased. In addition, we show that for low-multiplicity events the presence of jets can produce radial flow-like behavior. Motivated by our findings, we propose to perform a similar analysis using experimental data from RHIC and LHC.

Keywords: color reconnection, hydrodynamics, particle production, particle ratios, proton–proton collision, radial flow

1. Introduction

The study of particle production in high-multiplicity events in small collision systems at the LHC has revealed unexpected new collective-like phenomena. In particular, for high-multiplicity proton-proton (pp) and proton-lead (p-Pb) collisions, radial flow signals [1, 2], long-range angular correlations [3, 4], and the strangeness enhancement [5, 6, 7] have been reported. Those effects are well-known in heavy-ion collisions, where they are attributed to the existence of the strongly interacting Quark-Gluon Plasma (QGP) [8, 9, 10]. Understanding the phenomena is crucial because, for heavy-ion physics, pp and p-Pb collisions have been used as the baseline (“vacuum”) to extract the genuine QGP effects. However, it is worth mentioning that no jet quenching effects have been found so far in p-Pb collisions [11], suggesting that other mechanisms could also play a role in producing collective-like behavior in small collision systems [12, 13].

Hydrodynamic calculations reproduce many of the observations qualitatively [14]. However, it has also been found that multi-parton interactions (MPI) [15] and color reconnection (CR) as implemented in PYTHIA [16] produce radial flow patterns via boosted color strings [17]. Moreover, within the dilute-dense limit of the color glass condensate, it has been demonstrated that the physics of fluctuating color fields can generate azimuthal multi-particle correlations [18]; and the mass ordering of elliptic flow when the fragmentation implemented in PYTHIA is included [19]. The same observable has been studied using the multi-phase transport model [20], where the ridge structure can be generated assuming incoherent elastic scatterings of partons and the string melting mechanism. Other mechanisms like “color ropes”, which are formed by the fusion of color strings close in space, can increase both the strangeness production and the radial flow-like effects [21].

The measurements of the transverse momentum (p_T) spectra of identified particles as a function of event multiplicity in pp collisions at the LHC [5, 22] have shown that models fail to describe the data quantitatively. Therefore, the results of those comparisons alone are not enough to give desired information about the origin of the observed effects (i.e. radial flow-like patterns). In order to extract more information, we propose the implementation of a differential study based on the classification of the events according to event multiplicity and the jet content.

In the so-called MPI-based model of color reconnection [16], the interaction between scattered partons at soft and at hard p_T scales is imposed as follows. All gluons of low- p_T interactions can be inserted onto the colour-flow dipoles of a higher- p_T one, keeping the total string length as short as possible. Since the probability of having a hard scattering increases with the number of MPI, color reconnection can give a strong correlation between the radial flow-like patterns and the hard component of the collision [36] in high-multiplicity events.

On the contrary, in the scenario where the hydrodynamical evolution of the system is the prime mechanism, jets are not expected to strongly modify the radial flow patterns. Albeit hard partons cannot thermalize, momentum loss of jets could affect

the fluid dynamic evolution of the medium. However, the effect has been studied for heavy-ion collisions and it was found to give only a minor correction [23]. In the present paper we argue that by exploiting such a fundamental difference between both models, one might say whether or not the observed effects are driven by hydrodynamics. To this end, we propose a systematic study by analyzing the mid-rapidity ($|y| < 1$) inclusive p_T spectra of identified charged hadrons as a function of the mid-pseudorapidity ($|\eta| < 1$) event multiplicity (N_{ch}) and transverse momentum of the leading jet (p_T^{jet}). This study was carried out using PYTHIA 8.212 and EPOS 3.117 Monte Carlo (MC) event generators, from now on referred to as PYTHIA 8 and EPOS 3, respectively.

The paper is organized as follows: In section 2, some important features of the Monte Carlo event generators and the jet finder are outlined, with special emphasis on those aspects which are relevant in this study. In section 3, the results and discussion are presented. Finally, in section 4, the conclusions are given.

2. Simulation setup and Monte Carlo models

The studies were carried out for pp collisions at the centre-of-mass energy of $\sqrt{s} = 7$ TeV considering sets with and without the mechanism which produces radial flow patterns. To illustrate how PYTHIA 8 and EPOS 3 describe the experimental data measured by the ALICE Collaboration [2], Fig. 1 shows the proton-to-pion ratio for inelastic pp collisions at $\sqrt{s} = 7$ TeV. In the case of PYTHIA 8 shown in Fig. 1(a), as discussed in [17], the model shows a qualitative agreement with data, e.g., the bump in the proton-to-pion ratio, though the size of the effect is underestimated. The same level of accuracy is achieved by EPOS 3 which according to Fig. 1(b) overestimates the effect when hydrodynamics is included. So, in the end, we will compare models which still do not fully describe the data, but this is beside the point of our interest here. Instead, we shall study differences attributed to the fundamental underlying physics mechanisms which produce the observed radial flow effects.

The results are presented both for PYTHIA 8 and EPOS 3 using primary charged particles, defined as all charged particles produced in the collision including the products of strong and electromagnetic decays but excluding products of weak decays. Unless stated otherwise, no requirement on the minimum p_T of the particles is applied in any of the results. All MC generators use parton-to-hadron fragmentation approaches fitted to the experimental data—such as the Lund string [24] and area law hadronization [25] models.

For the results presented in this paper, we generated $\approx 10^2$ million inelastic events, including diffractive and non-diffractive components. A non-diffractive event includes a parton-parton interaction with a large momentum transfer (more than a few GeV/c). On the other hand, some inelastic collisions can be “diffractive”, in which a virtual particle (known as Pomeron) is responsible for the interaction. This sample was subsequently split into sub-samples based on the selection of charged particle multiplicity measured

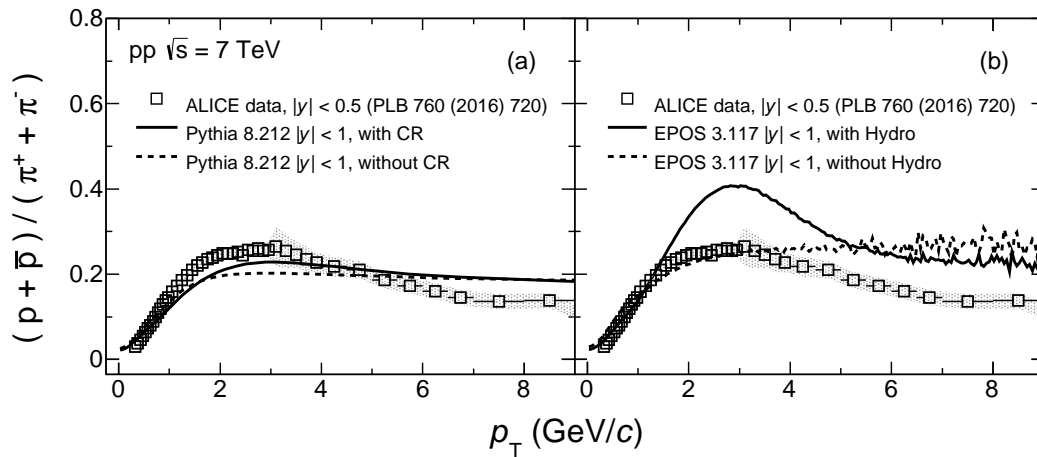


Figure 1: Proton-to-pion ratio as a function of p_T for inelastic pp collisions at $\sqrt{s} = 7$ TeV measured by the ALICE Collaboration [2]. Results are compared to models carried out with (a) PYTHIA 8 and (b) EPOS 3 event generators. Cases with and without the effect of color reconnection and hydrodynamics are plotted as solid and dashed lines, respectively

at mid-pseudorapidity and on the hardness of the event by imposing a cut on the jet transverse momentum (p_T^{jet}) found within the same acceptance.

2.1. EPOS 3 and hydrodynamics

EPOS 3 [26, 27] is a generator of complete events (soft + hard components) which contains hard scatterings and MPI. For high string densities, e.g. those achieved in high-multiplicity pp collisions, the model does not allow the strings to decay independently, instead, if energy density from string segments is high enough they fuse into the so-called “core” region, which evolves hydrodynamically. On the other hand, the low energy density region forms the “corona” which hadronizes using the unmodified string fragmentation.

The “core” region originates around 30% of the central particle production for an average pp collision at $\sqrt{s} = 7$ TeV, $\langle dN_{\text{ch}}/d\eta \rangle_{|\eta| < 2.4} \approx 6.25$. This fraction might reach $\approx 75\%$ for $\langle dN_{\text{ch}}/d\eta \rangle_{|\eta| < 2.4} \approx 20.8$ [28]. Concerning the hard component, the inclusive jet cross section for pp collisions at $\sqrt{s} = 0.2$ TeV obtained with EPOS 3 agrees within 5% and 4% with STAR data and NLO pQCD calculations, respectively [29]. Therefore, an analysis in EPOS 3 as a function of event multiplicity and leading jet transverse momentum is suitable to our needs.

To illustrate the effect of hydrodynamics on flow observables, Fig. 2 shows the proton-to-pion ratio as a function of p_T for different multiplicity classes, including also the inclusive case as a reference. Results are presented in intervals of z , defined as

$$z = \frac{dN_{\text{ch}}/d\eta}{\langle dN_{\text{ch}}/d\eta \rangle}, \quad (1)$$

where $\langle dN_{\text{ch}}/d\eta \rangle$ ($= 5.505$) is the average mid-rapidity particle density for inelastic pp collisions at $\sqrt{s} = 7$ TeV. It is important to mention that according to ALICE

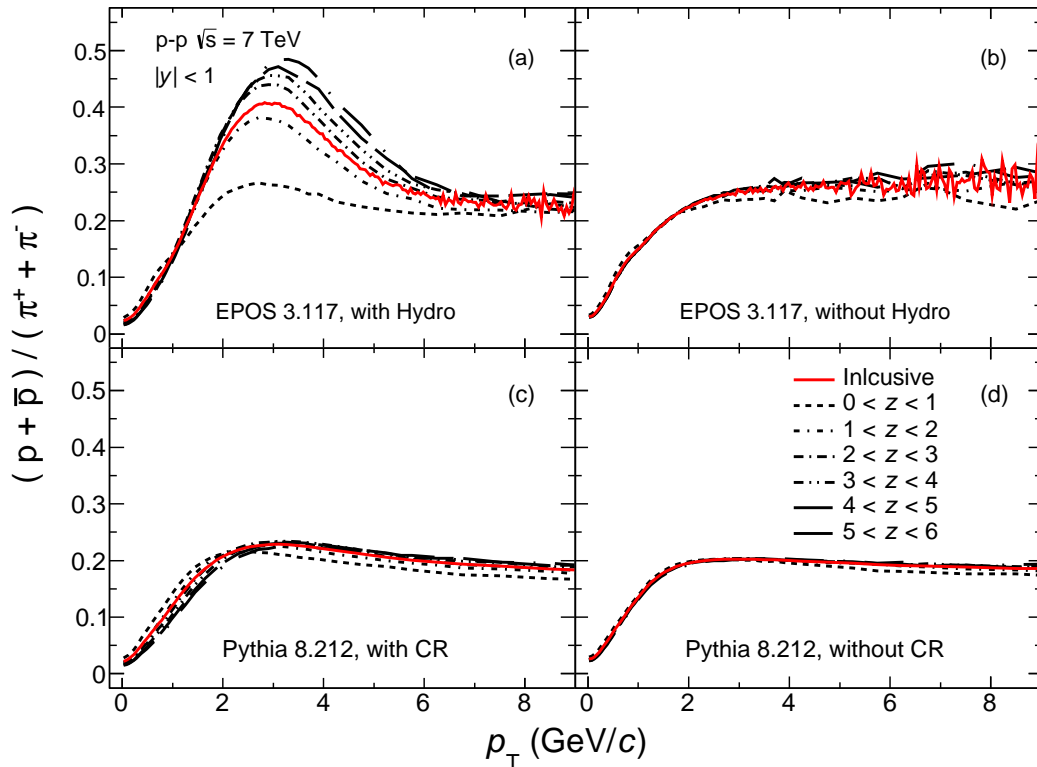


Figure 2: (Color online) Proton-to-pion ratio as a function of p_T for different multiplicity event classes. Results for pp collisions at $\sqrt{s} = 7$ TeV generated with EPOS 3 and PYTHIA 8 are presented. For PYTHIA 8 (EPOS 3) the ratios are displayed for simulations with and without color reconnection (hydrodynamical evolution of the system).

results [5] $\langle dN_{\text{ch}}/d\eta \rangle \sim 25$ is already large enough to see new phenomena in small systems, like the strangeness enhancement. For the simulations presented in this paper, such high multiplicity densities are achieved for $z > 4$. Fig. 2(a) shows the case when hydrodynamics is considered in the simulations. In this case, a clear evolution of the particle ratio with z can be observed, i.e. going from the lowest z to the highest z values the particle ratios exhibit a depletion (enhancement) for $p_T < 1$ GeV/ c ($1 < p_T < 6$ GeV/ c). This feature is usually attributed to radial flow which modifies the spectral shapes of the p_T distribution depending on the hadron mass. On the contrary, Fig. 2(b) shows the case without hydrodynamics, where the particle ratios do not evolve with multiplicity.

2.2. PYTHIA 8 and color reconnection

PYTHIA 8 [16] is a full event generator for pp collisions. For inelastic collisions, which is the main interest here, each collision is modeled via one or more parton-parton interactions. The full calculation involves leading-order (LO) pQCD $2 \rightarrow 2$ matrix elements, complemented with initial- and final-state parton radiation, multiple particle interactions, beam remnants and the Lund string fragmentation model. PYTHIA 8 also

has strong final-state parton interactions (implemented through the CR models [16]). In this work, we use the Monash 2013 tune [30] which has as default parametrisation the so-called MPI-based model of color reconnection. Such a model allows partons of each MPI system to form their own structure in color space and then, they are merged into the color structure of a higher p_T MPI system, with a probability \mathcal{P} given by:

$$\mathcal{P}(p_T) = \frac{(R \times p_{T0})^2}{(R \times p_{T0})^2 + p_T^2}, \quad (2)$$

where R is the reconnection range ($0 \leq R \leq 10$) and p_{T0} is the energy-dependent parameter used to damp the low- p_T divergence of the $2 \rightarrow 2$ QCD cross section.

Shown in the bottom row of Fig. 2 ((c) and (d) panels) are the proton-to-pion ratios for several z classes, with and without CR effects. It is worth noticing that compared to EPOS 3 (top row of Fig. 2) a similar indication for the radial flow effect is present in PYTHIA 8, but in this case, the radial flow-like behavior is attributed to color reconnection [17]. Also, it is remarkable that, in good approximation, with the CR option the magnitude of the peak is constant as a function of z .

2.3. FASTJET 3.1.3 and hardness of the event

Besides the multiplicity selection, we also classify events based on the transverse momentum (p_T^{jet}) of the produced jets. Per event, jets are reconstructed with the well-known anti- k_T algorithm implemented in FASTJET 3.1.3 [31], using charged and neutral particles, considering a cone radius of 0.4 and a minimum transverse momentum $p_{T,\text{min}}^{\text{jet}} = 5 \text{ GeV}/c$. The lower requirement on the jet p_T acts to suppress soft interactions by ensuring that at least one semi-hard scattering is present within the acceptance. In the following, the jet searching is done within a given pseudorapidity interval, which defines the maximum pseudorapidity of the jet. It is important to highlight that FASTJET is a well-known tool for jet reconstruction in heavy-ion collisions, where it has been extensively used, even in most central Pb–Pb collisions.

3. Results and discussion

3.1. Multiplicity dependence of the leading jet p_T

By running FASTJET (considering cone radius 0.4, $|\eta| < 1$ and $p_{T,\text{min}}^{\text{jet}} = 5 \text{ GeV}/c$) over the sample generated with PYTHIA 8 we obtain the results for the average mid-pseudorapidity densities, presented in Table 1.

Going from $\langle dN_{\text{ch}}/d\eta \rangle = 2.12$ to $\langle dN_{\text{ch}}/d\eta \rangle = 46.1$, the average leading jet p_T ranges from $7.09 \text{ GeV}/c$ up to $19.7 \text{ GeV}/c$. A similar behavior was found for the leading parton transverse momentum, obtained at mid-pseudorapidity, as a function of $\langle dN_{\text{ch}}/d\eta \rangle$. The effect is explained in the context of multi-partonic interactions because the probability of finding a hard parton is expected to be larger in high-multiplicity events (large average N_{mpi}) than in low-multiplicity events (small average N_{mpi}). This effect is also reflected in the behavior of the fraction of events having at least one jet with momentum above

$\left\langle \frac{dN_{\text{ch}}}{d\eta} \right\rangle_{ \eta <1}$	$\frac{dN_{\text{ch}}/d\eta}{\langle dN_{\text{ch}}/d\eta \rangle_{ \eta <1}} (\equiv z)$	$\langle p_{\text{T}}^{\text{jet}} \rangle_{ \eta <1}$ (GeV/c)	% of events with $p_{\text{T}}^{\text{jet}} > 5$ GeV/c
2.12	$0 < z < 1$	7.09	1.03
8.12	$1 < z < 2$	7.49	13.1
13.6	$2 < z < 3$	7.83	37.3
19.0	$3 < z < 4$	8.48	63.7
24.4	$4 < z < 5$	9.56	83.2
29.8	$5 < z < 6$	11.1	93.9
35.2	$6 < z < 7$	13.2	98.2
40.6	$7 < z < 8$	16.1	99.5
46.1	$8 < z < 9$	19.7	99.8

Table 1: Charged-particle pseudorapidity densities at central pseudorapidity ($|\eta| < 1$), for pp collisions at $\sqrt{s} = 7$ TeV simulated with PYTHIA 8 having jets with p_{T} above 5 GeV/c in the same pseudorapidity region. The multiplicity classes are presented along the leading jet p_{T} and the fraction of events where a jet with p_{T} above 5 GeV/c was identified.

5 GeV/c. In the second column of Tab 1 we included the corresponding event multiplicity class defined by Eq. 1 in comparison to the other measured variables. For the presented results we considered events having z from the lowest possible value ($0 < z < 1$) up to $5 < z < 6$. One can see that for the highest considered z interval ($5 < z < 6$) more than 90% of the events contain jets with $p_{\text{T}}^{\text{jet}} > 5$ GeV/c. This feature is simply the result of the selection bias, i.e. the higher the multiplicity at mid-pseudorapidity the higher the probability to find jets within the same η region.

3.2. Proton-to-pion ratio as a function of z and $p_{\text{T}}^{\text{jet}}$

Figure 3 shows the proton-to-pion ratio as a function of p_{T} for event classes with low and high z . Regarding the low- z case ($0 < z < 1$), results indicate that for $5 < p_{\text{T}}^{\text{jet}} < 10$ GeV/c the ratios exhibit an enhancement at $p_{\text{T}} \approx 3$ GeV/c for both EPOS 3 and PYTHIA 8. If the $p_{\text{T}}^{\text{jet}}$ is increased then the position of the observed peak is shifted to higher p_{T} . This observation suggests that the peak is not an exclusive effect of radial flow (as suggested by Fig. 2), but also a feature of the fragmentation. It is worth noticing that the same effect has been observed in ALICE data, where the jet hadrochemistry has been measured in minimum bias pp collisions at $\sqrt{s} = 7$ TeV [32].

Also shown in Fig. 3 the multiplicity class $5 < z < 6$, where we see that the maximum of the proton-to-pion ratio increases with increasing multiplicity, showing significantly stronger behavior for EPOS 3 than for PYTHIA 8. In EPOS 3, the event class $5 < p_{\text{T}}^{\text{jet}} < 10$ GeV/c exhibits an enhancement of the $(p + \bar{p})/(\pi^+ + \pi^-)$ ratio with respect to the inclusive case shown in Fig. 2 without any selection on $p_{\text{T}}^{\text{jet}}$. Going to higher $p_{\text{T}}^{\text{jet}}$, the position of the peak is shifted to lower p_{T} values and the magnitude

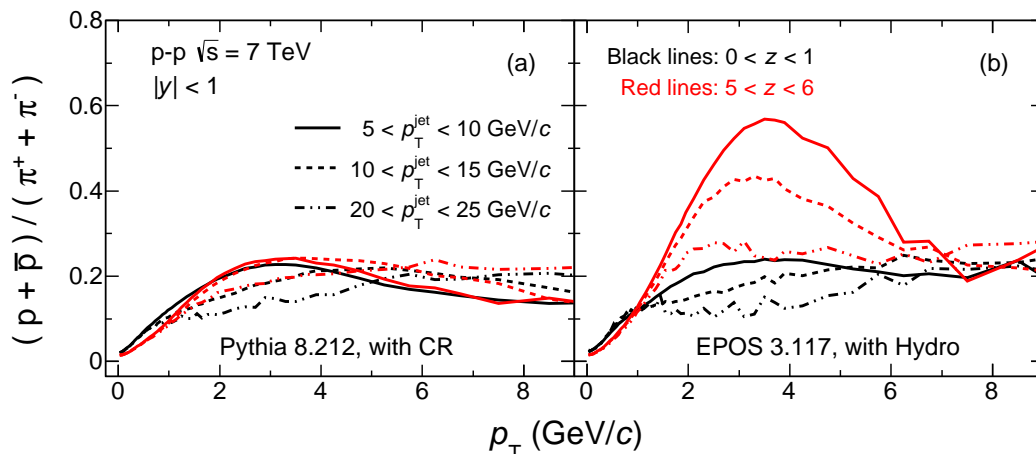


Figure 3: (Color online) Proton-to-pion ratio as a function of p_T for two multiplicity classes, $0 < z < 1$ (black lines) and $5 < z < 6$ (red lines); and for different p_T^{jet} intervals. Results are shown for both (a) PYTHIA 8 and (b) EPOS 3.

of the peak is significantly smaller than in the inclusive case. In contrast, the effect is quantitatively and qualitatively different in PYTHIA 8. Namely, the height of the peak is approximately independent of the increase of p_T^{jet} , instead, there is a moderate shift towards higher p_T . In EPOS 3, the effect vanishes when hydrodynamical effects are switched off—in a similar way as seen in Fig. 2(b). Therefore, it can be a consequence of the “core-corona” separation, where low-momentum partons are more likely forming the “core” region. It is worth mentioning that this difference between the two event classes could contribute to the differences observed in the hadrochemistry measured in the so-called “bulk” (outside the jet peak) and the jet regions in p–Pb and Pb–Pb collisions at the LHC [33, 34]. To summarize, an analysis of data as a function of event multiplicity and the hardness of the event provides a more powerful tool for testing the aforementioned models than the one which considers selection based only on event multiplicity.

3.3. Blast-wave model fits

Color reconnection, without any hydrodynamical component, produces radial flow-like patterns in events simulated with PYTHIA 8, as shown in Ref. [17]. Such a conclusion was based on the good agreement between the Boltzmann–Gibbs blast-wave model and the p_T spectra of different particle species. The blast-wave model describes a locally thermalised medium which experiences a collective expansion with a common velocity field and undergoing an instantaneous common freeze-out [35]. The functional form of the model is given by:

$$\frac{dN}{p_T dp_T} \propto \int_0^R r dr m_T I_0 \left(\frac{p_T \sinh \rho}{T_{\text{kin}}} \right) K_1 \left(\frac{m_T \cosh \rho}{T_{\text{kin}}} \right), \quad (3)$$

where K_1 and I_0 are the modified Bessel functions, and T_{kin} is the kinetic freeze-out

temperature. On the other hand, $\rho = \tanh^{-1}(\beta_T)$, where β_T is the radial profile of the transverse expansion velocity.

From the simultaneous fit of the blast-wave model to the p_T spectra of different particle species we extract two parameters: T_{kin} and $\langle\beta_T\rangle$. In the current study we considered the p_T ranges: $0.5 < p_T < 1.0 \text{ GeV}/c$, $0.3 < p_T < 1.5 \text{ GeV}/c$ and $0.8 < p_T < 2.0 \text{ GeV}/c$ to fit the model to the p_T distributions of charged pions, kaons and (anti)protons, respectively. The specific selection of the p_T ranges mentioned above was successfully applied in our previous studies [36] where the parametrizations, obtained from the fits, described within 10% the strange and multi-strange hadron p_T spectra.

For pp collisions at $\sqrt{s} = 7 \text{ TeV}$ simulated with PYTHIA 8, Fig. 4 shows the p_T spectra of charged pions, kaons and (anti)protons for two multiplicity classes, $0 < z < 1$ (upper panel (a)) and $5 < z < 6$ (lower panel (b)), being each one split into three specific subclasses based on the selection of the jet transverse momentum, p_T^{jet} . The first subclass is treated as a baseline since no jets at mid-pseudorapidity are found; it is compared with samples in which low (5–10 GeV/c) and high (20–25 GeV/c) p_T jets are produced. For a given average multiplicity z class and jet transverse momentum p_T^{jet} interval two cases are considered: with and without color reconnection.

There are some interesting observations one might read off from the results of this analysis. Firstly, we concentrate on results obtained from PYTHIA 8 simulations, since we already know we might expect the presence of radial flow patterns. Then we shall be examining the results produced by EPOS 3.

Even at extremely low multiplicity ($0 < z < 1$), where color reconnection effects are negligible, it is possible to find an event class where the radial flow-like patterns pop up. Especially, in events having $p_T^{\text{jet}} > 5 \text{ GeV}/c$ the p_T distributions of identified hadrons are better described by the blast-wave model than in those without jets. Looking at differences between the model fit and the MC result in terms of ratios (shown in the bottom rows of Fig. 4(a)) one can see a smoothening trend with p_T when going towards higher p_T^{jet} which is hardly visible for pions but more pronounced for kaons and (anti)protons. This behavior is also supported by the reduction on the reduced χ^2 values: fit results give $\chi^2/\text{n.d.f} = 3.28$ (4.65) for events without jets and $\chi^2/\text{n.d.f} = 1.51$ (1.09) for events including jets with $20 < p_T^{\text{jet}} < 25 \text{ GeV}/c$ for the case with (without) color reconnection, respectively.

It is worth mentioning that recently the CMS Collaboration has reported that in low-multiplicity pp events, the elliptic flow Fourier harmonic is not zero [4], supporting the idea that other mechanisms could produce the collective-like behavior.

In high-multiplicity events ($5 < z < 6$), again, examining the relative differences between the spectra and the fits, the overall agreement between the spectra and the blast-wave fits shows a smaller dependence with p_T^{jet} . The blast-wave model fits give a slightly worse description of the spectra when CR is not included in the simulation – even if a jet with $p_T^{\text{jet}} > 5 \text{ GeV}/c$ is produced at mid-rapidity – than for the case with the inclusion of CR. The ratios of spectra (simulated with CR) to blast-wave model show a modest smoothening trend with increasing p_T^{jet} while those without CR stay approximately p_T^{jet} -

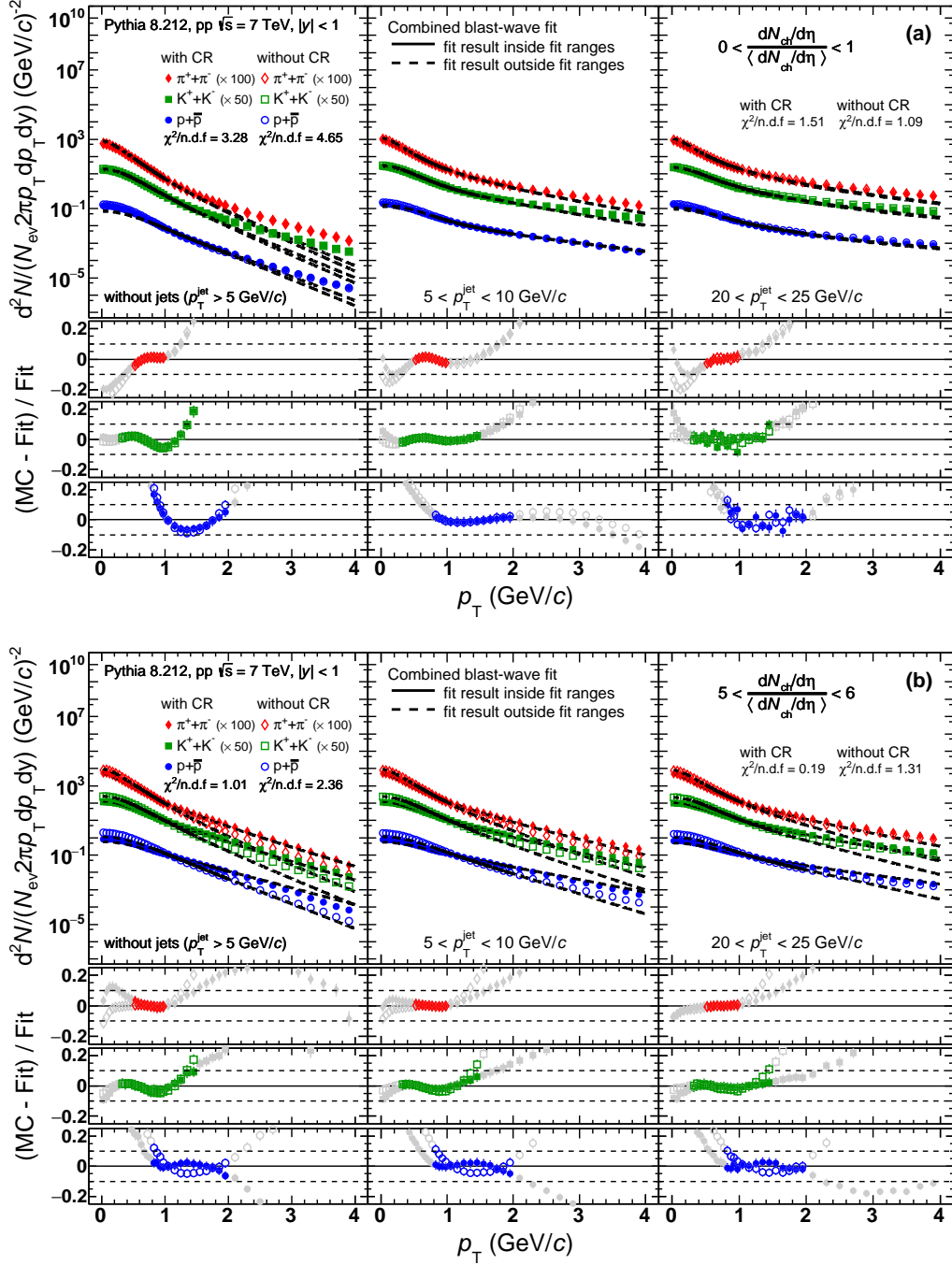


Figure 4: (Color online) Transverse momentum distributions of charged pions, kaons and (anti)protons for (a) low- and (b) high-multiplicity pp collisions at $\sqrt{s} = 7$ TeV generated with PYTHIA 8. For each multiplicity class, three sub-samples are shown, from left to right, events without a leading jet with $p_T^{\text{jet}} > 5$ GeV/c, with $5 < p_T^{\text{jet}} < 10$ GeV/c and with $20 < p_T^{\text{jet}} < 25$ GeV/c, respectively. Results for the cases with and without color reconnection (CR) are plotted with full and empty markers, respectively. The parametrizations obtained from the simultaneous blast-wave fits are shown as solid lines. The deviation of the p_T spectrum from the blast-wave model is shown in the bottom panels, indicating the fitting range using colored markers.

independent. These observations are confirmed by the fit qualities in terms of reduced χ^2 values: $\chi^2/\text{n.d.f} = 1.01$ (2.36) for events without jets and $\chi^2/\text{n.d.f} = 0.19$ (1.31) for events including jets ($20 < p_T^{\text{jet}} < 25 \text{ GeV}/c$) for the case with (without) color reconnection. The observed effects just reflect the fact that in PYTHIA 8 the interaction between jets and the underlying event is crucial for generating a collective-like behavior.

Shown in Fig. 5 the results obtained from the blast-wave analysis of the p_T spectra simulated with EPOS 3. In general, the observed effects are quite similar to those shown for PYTHIA 8 (Fig. 4), even though the statistics is notably limited for jets with higher p_T^{jet} . In low-multiplicity events with no jets produced (Fig. 5(a) left column) charged kaons show worse model description than those seen for PYTHIA 8 (Fig. 4(a) left column) which are similar in shape and magnitude to (anti)protons. Also, the corresponding χ^2 values are remarkably higher in events without jets simulated with (without) hydrodynamical evolution, i.e. $\chi^2/\text{n.d.f} = 5.55$ (9.18), than in those simulated with (and without) color reconnection in PYTHIA 8.

Low- z p_T spectra in EPOS 3 for all particle species are better described by the blast-wave model. It is noteworthy that it is hard to make strong conclusion for the highest p_T^{jet} event class due to its limited statistics, but the points tend to show similar behavior compared to the former event class with jets $5 < p_T^{\text{jet}} < 10 \text{ GeV}/c$.

In high- z events, the model description of the p_T spectra show the same behavior seen in PYTHIA 8. Namely, with the inclusion of hydrodynamical component in the simulation, the agreement is somewhat better for the case with the hydro option. Besides that, there is a clear dependence seen between the two options (shown with full and open markers) also for charged pions and kaons. The p_T spectra have a weak p_T^{jet} -dependent behavior and their agreement with the blast-wave model improves towards higher p_T^{jet} , with the change of $\chi^2/\text{n.d.f}$ from 1.33 (6.74) to 0.77 (1.29) as we consider events with (without) setting hydro option, respectively.

To quantify the importance of jets in events where flow patterns are generated with hydrodynamics or color reconnection, Fig. 6 shows the correlation between the blast-wave parameters T_{kin} and $\langle\beta_T\rangle$. Results are shown for different z multiplicity classes which are indicated by different marker sizes and increase from low to high multiplicity. Besides the multiplicity selection, also shown the case when we consider the selection on the hardness of the event by imposing a cut on p_T^{jet} .

In continuation to the previous observation based on the fit qualities for various event classes in PYTHIA 8 and in EPOS 3, by looking at the evolution of the blast-wave fit parameters in terms of z and p_T^{jet} we see that:

- For events containing jets and being in the same multiplicity class (indicated by the same marker size), $\langle\beta_T\rangle$ increases with respect to the case without any selection on the hardness (inclusive case indicated by open markers). This is a somewhat natural consequence of the auto-correlation bias due to hard partons inducing a large boost. Moreover, by looking at, the case of jets with $20 < p_T^{\text{jet}} < 25 \text{ GeV}/c$ and the highest multiplicity class ($5 < z < 6$), the effect is weaker in EPOS 3 ($\approx 0.6\%$) than in PYTHIA 8 ($\approx 6.8\%$). Implicitly, this is also illustrated in the

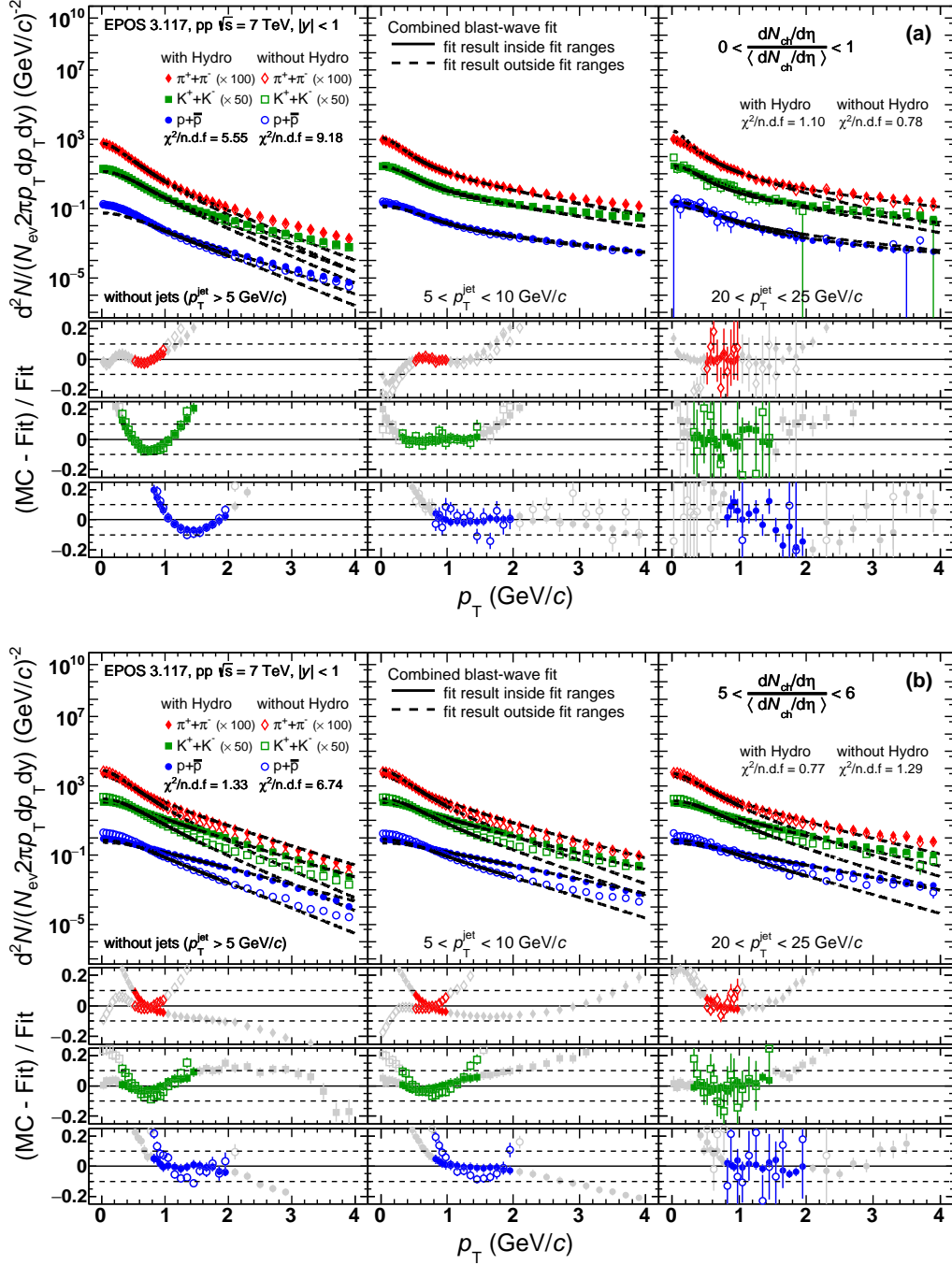


Figure 5: (Color online) Transverse momentum distributions of charged pions, kaons and (anti)protons for (a) low- and (b) high-multiplicity pp collisions at $\sqrt{s} = 7 \text{ TeV}$ generated with EPOS 3. For each multiplicity class, three sub-samples are shown. From left to right, events without a leading jet with $p_T^{\text{jet}} > 5 \text{ GeV}/c$, with $5 < p_T^{\text{jet}} < 10 \text{ GeV}/c$ and with $20 < p_T^{\text{jet}} < 25 \text{ GeV}/c$, respectively. Results for the cases with and without hydrodynamics (hydro) are plotted with full and empty markers, respectively. The parametrizations obtained from the simultaneous blast-wave fits are shown as solid lines. The deviation of the p_T spectrum from the blast-wave model is shown in the bottom panels, indicating the fitting range using colored markers.

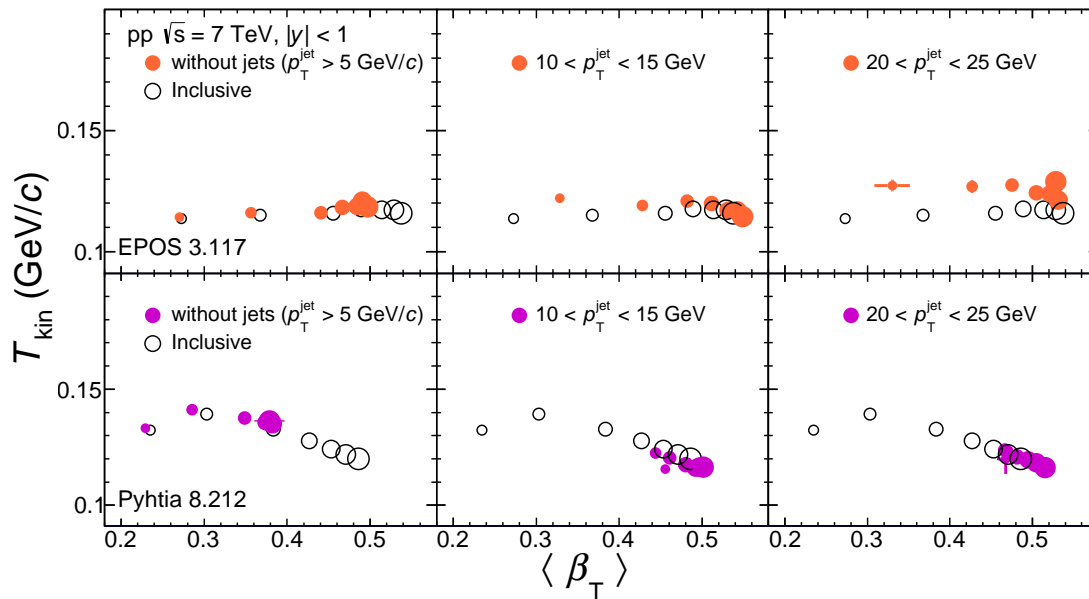


Figure 6: (Color online) Correlation between two fit parameters obtained from the blast-wave analysis, the kinetic temperature (T_{kin}) and the average transverse expansion velocity ($\langle \beta_T \rangle$) of the system. Results for pp collisions at $\sqrt{s} = 7 \text{ TeV}$ simulated with EPOS 3 and PYTHIA 8 are presented in the top and the bottom rows, respectively. The size of the markers increases with the event multiplicity. Results with (full markers) and without (empty markers) a selection on p_T^{jet} are compared.

smaller multiplicity dependence of $\langle \beta_T \rangle$ obtained in PYTHIA 8 than that observed in EPOS 3 where the role of jets is considerably weaker.

- In low- z events (as explained earlier) the p_T spectra deviate from the blast-wave model—in contrast to events with higher z —and the agreement improves with increasing p_T^{jet} . In connection to those observations, taking low- z parameters in Fig. 6 we see a weak p_T^{jet} dependence as a function of $\langle \beta_T \rangle$ in EPOS 3 whereas in PYTHIA 8 for a given low- z class events with increasing p_T^{jet} experience a larger radial flow velocity $\langle \beta_T \rangle$. In addition, one sees that in PYTHIA 8 the larger the $\langle \beta_T \rangle$ the smaller the T_{kin} reaching at slightly smaller values for the highest z class than those in EPOS 3 where the T_{kin} dependence of $\langle \beta_T \rangle$ is almost flat.

4. Conclusions

In this work, we have presented a study using two event generators, EPOS 3 and PYTHIA 8, exploring an observable which is aimed at ruling out or validating the underlying physics mechanism (hydrodynamics or color reconnection) generating radial flow patterns in pp collisions. Specifically, we exploit the fact that, by construction, color reconnection produces a strong coupling between the hard (hard partons) and soft (soft and semi-hard partons) components of the interaction. To this end, we have studied the p_T spectra of charged pions, kaons and (anti)protons as a function of the

event multiplicity and the transverse momentum of the leading jet. Our main findings can be summarized as follows:

- The multiplicity dependence of the proton-to-pion particle ratios show a depletion for $p_T \lesssim 1 - 2 \text{ GeV}/c$ and an enhancement above, ending up with a bump at around $p_T \approx 3 \text{ GeV}/c$. Apart from the multiplicity selection, a more differential classification was done by using the leading jet transverse momentum (p_T^{jet}). At extremely low multiplicity, it is possible to find a subclass of events where radial flow patterns arise—despite the fact that at very low multiplicity—hydrodynamics cannot be applied and color reconnection effects are small. This feature is present both for PYTHIA 8 and EPOS 3.
- In high-multiplicity events the particle composition is very different in PYTHIA 8 and EPOS 3 which is nicely visible on the proton-to-pion ratios when multiplicity and p_T^{jet} vary. In EPOS 3 the magnitude of the bump significantly increases with decreasing p_T^{jet} . On the contrary, in PYTHIA 8 the height of the peak does not change with p_T^{jet} .
- Furthermore, the agreement between the blast-wave model and the charged pion, kaon and (anti)proton spectra in events classified using multiplicity and p_T^{jet} , significantly improves with the increase of the leading jet p_T . More importantly, this agreement was found to be the best in low-multiplicity events having jets, suggesting the presence of the collective-like behavior caused by jets.
- The multiplicity and jet transverse momentum dependence of the blast-wave fit parameters, i.e. the average transverse expansion velocity ($\langle\beta_T\rangle$) and the kinetic temperature (T_{kin}), also shows effects which can be used to discriminate between different models. It is found that the multiplicity dependence of $\langle\beta_T\rangle$ is more affected by jets in PYTHIA 8 than in EPOS 3.

Acknowledgments

We acknowledge Gergely Gábor Barnaföldi, Peter Christiansen, Eleazar Cuautle, Arturo Fernández and Guy Paic for the critical reading of the manuscript and the valuable discussion and suggestions. We also acknowledge Klaus Werner for allowing us the usage of EPOS 3.117 and for the useful instructions.

Support for this work has been received from CONACYT under the grant No. 260440; from DGAPA-UNAM under PAPIIT grant IA102515. In addition, this work was supported by Hungarian OTKA grants NK106119, K120660 and NIH TET 12 CN-1-2012-0016.

References

- [1] B. B. Abelev, et al., Multiplicity dependence of pion, kaon, proton and lambda production in p–Pb collisions at $\sqrt{s_{\text{NN}}} = 5.02 \text{ TeV}$, *Phys. Lett.* **B728** (2014) 25–38. [arXiv:1307.6796](https://arxiv.org/abs/1307.6796), [doi:10.1016/j.physletb.2013.11.020](https://doi.org/10.1016/j.physletb.2013.11.020).

- [2] J. Adam, et al., Multiplicity dependence of charged pion, kaon, and (anti)proton production at large transverse momentum in p–Pb collisions at $\sqrt{s_{\text{NN}}} = 5.02$ TeV, *Phys. Lett.* **B760** (2016) 720–735. [arXiv:1601.03658](#), [doi:10.1016/j.physletb.2016.07.050](#).
- [3] B. B. Abelev, et al., Long-range angular correlations of π , K and p in p–Pb collisions at $\sqrt{s_{\text{NN}}} = 5.02$ TeV, *Phys. Lett.* **B726** (2013) 164–177. [arXiv:1307.3237](#), [doi:10.1016/j.physletb.2013.08.024](#).
- [4] V. Khachatryan *et al.* [CMS Collaboration], Evidence for collectivity in pp collisions at the LHC, *Phys. Lett. B* **765**, 193 (2017) [arXiv:1606.06198](#), [doi:10.1016/j.physletb.2016.12.009](#).
- [5] J. Adam *et al.* [ALICE Collaboration], Multiplicity-dependent enhancement of strange and multi-strange hadron production in proton-proton collisions at $\sqrt{s} = 7$ TeV, [arXiv:1606.07424](#).
- [6] J. Adam, et al., Multi-strange baryon production in p–Pb collisions at $\sqrt{s_{\text{NN}}} = 5.02$ TeV, *Phys. Lett.* **B758** (2016) 389–401. [arXiv:1512.07227](#), [doi:10.1016/j.physletb.2016.05.027](#).
- [7] V. Khachatryan *et al.* [CMS Collaboration], Multiplicity and rapidity dependence of strange hadron production in pp, pPb, and PbPb collisions at the LHC, *Phys. Lett. B* **768**, 103 (2017) [arXiv:1605.06699](#), [doi:10.1016/j.physletb.2017.01.075](#).
- [8] R. Bala, I. Bautista, J. Bielcikova, A. Ortiz, Heavy-ion physics at the LHC: Review of Run I results, *Int. J. Mod. Phys.* **E25** (2016) 1642006. [arXiv:1605.03939](#), [doi:10.1142/S0218301316420064](#).
- [9] B. B. Abelev, et al., Production of charged pions, kaons and protons at large transverse momenta in pp and Pb–Pb collisions at $\sqrt{s_{\text{NN}}} = 2.76$ TeV, *Phys. Lett.* **B736** (2014) 196–207. [arXiv:1401.1250](#), [doi:10.1016/j.physletb.2014.07.011](#).
- [10] J. Adam, et al., Centrality dependence of the nuclear modification factor of charged pions, kaons, and protons in Pb–Pb collisions at $\sqrt{s_{\text{NN}}} = 2.76$ TeV, *Phys. Rev.* **C93** (3) (2016) 034913. [arXiv:1506.07287](#), [doi:10.1103/PhysRevC.93.034913](#).
- [11] J. Adam, et al., Measurement of charged jet production cross sections and nuclear modification in p–Pb collisions at $\sqrt{s_{\text{NN}}} = 5.02$ TeV, *Phys. Lett.* **B749** (2015) 68–81. [arXiv:1503.00681](#), [doi:10.1016/j.physletb.2015.07.054](#).
- [12] A. Ortiz, Mean p_{T} scaling with m/n_q at the LHC: Absence of (hydro) flow in small systems?, *Nucl. Phys.* **A943** (2015) 9–17. [arXiv:1506.00584](#), [doi:10.1016/j.nuclphysa.2015.08.003](#).
- [13] B. G. Zakharov, Flavor dependence of jet quenching in pp collisions and its effect on R_{AA} for heavy mesons, *JETP Lett.* **103** (6) (2016) 363–368. [arXiv:1509.07020](#), [doi:10.1134/S0021364016060126](#).
- [14] P. Bozek, W. Broniowski, G. Torrieri, Mass hierarchy in identified particle distributions in proton–lead collisions, *Phys. Rev. Lett.* **111** (2013) 172303. [arXiv:1307.5060](#), [doi:10.1103/PhysRevLett.111.172303](#).
- [15] T. Sjostrand, M. van Zijl, A Multiple Interaction Model for the Event Structure in Hadron Collisions, *Phys. Rev. D* **36** (1987) 2019. [doi:10.1103/PhysRevD.36.2019](#).
- [16] T. Sjostrand, S. Ask, J. R. Christiansen, R. Corke, N. Desai, P. Ilten, S. Mrenna, S. Prestel, C. O. Rasmussen, P. Z. Skands, An Introduction to PYTHIA 8.2, *Comput. Phys. Commun.* **191** (2015) 159–177. [arXiv:1410.3012](#), [doi:10.1016/j.cpc.2015.01.024](#).
- [17] A. Ortiz Velasquez, P. Christiansen, E. Cuautle Flores, I. Maldonado Cervantes and G. Pai, Color Reconnection and Flowlike Patterns in *pp* Collisions, *Phys. Rev. Lett.* **111**, no. 4, 042001 (2013) [arXiv:1303.6326](#), [doi:10.1103/PhysRevLett.111.042001](#).
- [18] T. Lappi, B. Schenke, S. Schlichting, R. Venugopalan, Tracing the origin of azimuthal gluon correlations in the color glass condensate, *JHEP* **01** (2016) 061. [arXiv:1509.03499](#), [doi:10.1007/JHEP01\(2016\)061](#).
- [19] B. Schenke, S. Schlichting, P. Tribedy and R. Venugopalan, Mass ordering of spectra from fragmentation of saturated gluon states in high multiplicity proton-proton collisions, *Phys. Rev. Lett.* **117**, no. 16, 162301 (2016) [arXiv:1607.02496](#), [doi:10.1103/PhysRevLett.117.162301](#).
- [20] G.-L. Ma, A. Bzdak, Long-range azimuthal correlations in proton–proton and proton-nucleus collisions from the incoherent scattering of partons, *Phys. Lett.* **B739** (2014) 209–213.

- arXiv:1404.4129, doi:10.1016/j.physletb.2014.10.066.
- [21] C. Bierlich, G. Gustafson, L. Lonnblad, A. Tarasov, Effects of Overlapping Strings in pp Collisions, *JHEP* **03** (2015) 148. arXiv:1412.6259, doi:10.1007/JHEP03(2015)148.
- [22] S. Chatrchyan, et al., Study of the inclusive production of charged pions, kaons, and protons in pp collisions at $\sqrt{s} = 0.9, 2.76, \text{ and } 7$ TeV, *Eur. Phys. J.* **C72** (2012) 2164. arXiv:1207.4724, doi:10.1140/epjc/s10052-012-2164-1.
- [23] S. Floerchinger and K. Zapp, Hydrodynamics and Jets in Dialogue, *Eur. Phys. J.* **C74** (2014) 12. arXiv:1407.1782v1, doi:10.1140/epjc/s10052-014-3189-4.
- [24] B. Andersson, G. Gustafson, G. Ingelman, T. Sjostrand, Parton Fragmentation and String Dynamics, *Phys. Rept.* **97** (1983) 31–145. doi:10.1016/0370-1573(83)90080-7.
- [25] X. Artru, G. Mennessier, String model and multiproduction, *Nucl. Phys.* **B70** (1974) 93–115. doi:10.1016/0550-3213(74)90360-5.
- [26] K. Werner, B. Guiot, I. Karpenko, T. Pierog, Analysing radial flow features in p–Pb and p–p collisions at several TeV by studying identified particle production in EPOS3, *Phys. Rev.* **C89** (6) (2014) 064903. arXiv:1312.1233, doi:10.1103/PhysRevC.89.064903.
- [27] K. Werner, I. Karpenko, T. Pierog, M. Bleicher, K. Mikhailov, Evidence for hydrodynamic evolution in proton–proton scattering at 900 GeV, *Phys. Rev.* **C83** (2011) 044915. arXiv:1010.0400, doi:10.1103/PhysRevC.83.044915.
- [28] T. Martin, P. Skands, S. Farrington, Probing Collective Effects in Hadronisation with the Extremes of the Underlying Event, *Eur. Phys. J.* **C76** (5) (2016) 299. arXiv:1603.05298, doi:10.1140/epjc/s10052-016-4135-4.
- [29] S. Porteboeuf, T. Pierog, K. Werner, Producing Hard Processes Regarding the Complete Event: The EPOS Event Generator, *Proceedings, 45th Rencontres de Moriond on Electroweak Interactions and Unified Theories, 2010, 135–140, vol. 2.* arXiv:1006.2967.
- [30] P. Skands, S. Carrazza, J. Rojo, Tuning PYTHIA 8.1: the Monash 2013 Tune, *Eur. Phys. J.* **C74** (8) (2014) 3024. arXiv:1404.5630, doi:10.1140/epjc/s10052-014-3024-y.
- [31] M. Cacciari, G. P. Salam, G. Soyez, FastJet User Manual, *Eur. Phys. J.* **C72** (2012) 1896. arXiv:1111.6097, doi:10.1140/epjc/s10052-012-1896-2.
- [32] X. Lu, Measurement of hadron composition in charged jets from pp collisions with the ALICE experiment, *Nucl. Phys.* **A931** (2014) 428–432. arXiv:1407.8385, doi:10.1016/j.nuclphysa.2014.08.003.
- [33] M. Veldhoen, p/ π Ratio in Di-Hadron Correlations, *Nucl. Phys.* **A910-911** (2013) 306–309. arXiv:1207.7195, doi:10.1016/j.nuclphysa.2012.12.103.
- [34] X. Zhang, K_S^0 and Λ production in charged particle jets in p–Pb collisions at $\sqrt{s_{NN}} = 5.02$ TeV with ALICE, *Nucl. Phys.* **A931** (2014) 444–448. arXiv:1408.2672, doi:10.1016/j.nuclphysa.2014.08.102.
- [35] E. Schnedermann, J. Sollfrank, U. W. Heinz, Thermal phenomenology of hadrons from 200-A/GeV S+S collisions, *Phys. Rev.* **C48** (1993) 2462–2475. arXiv:nucl-th/9307020, doi:10.1103/PhysRevC.48.2462.
- [36] A. Ortiz, G. Paić, E. Cuautle, Mid-rapidity charged hadron transverse sphericity in pp collisions simulated with Pythia, *Nucl. Phys.* **A941** (2015) 78–86. arXiv:1503.03129, doi:10.1016/j.nuclphysa.2015.05.010.